Tightly Coupled GPS/INS Integration for Differential Carrier Phase Navigation Systems Using Decentralized Estimation

Steven E. Langel, Samer M. Khanafseh, Fang-Cheng Chan, and Boris S. Pervan
Illinois Institute of Technology, Chicago, IL

ABSTRACT

Much research has been conducted in the area of tightly coupled GPS/INS, and this work has resulted in a vast array of navigation algorithms. A common theme of these methods is that they operate on low rate GPS ranging measurements of code and carrier phase together with high rate raw inertial measurements, such as specific force and inertial angular velocity. For stand-alone (i.e., non-differential) GPS navigation applications, high data rate INS outputs can be properly accommodated with today's computer processors. For relative (i.e., differential) GPS navigation applications, the optimal analogous solution would be for the mobile user to have access to the reference station's raw inertial measurements along with its own. However, due to communication bandwidth limitations, it is generally not possible to broadcast high data rate inertial navigation data. In response, an alternative tightly-coupled, differential GPS/INS navigation system is developed here using a decentralized Kalman filtering approach, which can operate at manageable broadcast data rates.

The essence of the concept is that both the user and reference platforms run their own stand-alone, tightly coupled GPS/INS Kalman filter algorithms to produce estimates of position, velocity and attitude (PVA). The reference station broadcasts these state estimates at a low data rate to a differential Kalman filter onboard the user platform, which together with the corresponding user-generated state estimates, constructs nominal values of the relative position and relative velocity states. Based on this nominal state trajectory, the filter then incorporates low rate-GPS differential code and carrier phase measurements to estimate the deviation of the true state from the nominal state.

The estimation performance of the decentralized differential Kalman filtering scheme is compared to tightly coupled architectures where high rate raw inertial measurements are hypothetically available. An example application of the decentralized differential filter, an aircraft executing a figure eight flight maneuver, is specifically considered in this analysis for quantitative performance comparisons.

INTRODUCTION

The integration of GPS and inertial sensors has been exploited in many areas of navigation research, especially situations involving periods of satellite blockage. The ability of the inertial navigation system to coast through periods of GPS unavailability can result in robust navigation algorithms for applications demanding high accuracy, integrity and continuity.

For the stand-alone user, a wide variety of integration schemes are available. In general, these can be classified as loosely coupled, tightly coupled or ultra-tightly coupled. Tightly coupled architectures are generally preferred over loosely coupled designs because they allow a navigation solution to be computed even if the number of GPS satellites falls below four. However, if GPS signal vulnerability is an issue, the user may opt for a deeply coupled approach, in which INS measurements are used to directly aid the GPS receiver tracking loops. A more detailed account of the different integration architectures can be found in [6]. In the remaining sections of this paper, the focus will be on tightly coupled integration schemes.

With the capabilities of today's processors, it is possible to design real time navigation algorithms for the stand-alone user that can accommodate the high rate inertial sensor data. Prior research work has addressed the problem of tight coupling an inertial navigation system with GPS for applications in which the reference station is stationary [5]. For this special case, it is not necessary to have access to high rate inertial sensor data from the reference station. In this work, we consider applications in which the reference station is allowed to be mobile. Under this scenario, it is necessary to know the position

and velocity of the reference station in order to ensure that a high accuracy, high integrity estimate of the relative position vector can be computed.

One approach to obtaining this information is to process raw inertial measurements from the reference station at the user platform. However, this requires high data rate inertial navigation data to be broadcast to the user platform, which may not be possible due to communication bandwidth limitations. In response, an alternative tightly-coupled, differential GPS/INS navigation system is developed here using a decentralized Kalman filtering approach, which can operate at manageable broadcast data rates.

The essence of the concept is that both the user and reference stations run their own stand-alone, tightly coupled GPS/INS Kalman filter algorithms to produce estimates of position, velocity and attitude (PVA). The reference station broadcasts these state estimates at a low data rate to a differential Kalman filter onboard the user platform, which together with the corresponding user-generated state estimates, constructs nominal values of the relative position and relative velocity states. Based on this nominal state trajectory, the filter then incorporates low rate-GPS differential code and carrier phase measurements to estimate the deviation of the true state from the nominal state.

RUDIMENTS OF TIGHTLY COUPLED GPS/INS

Before describing the end state architecture, let's first consider how to design a tightly coupled GPS/INS algorithm for a stand-alone user. In this situation, the user is primarily interested in estimating his/her absolute position in an Earth centered Earth fixed (ECEF) coordinate system. The theory developed in this section will be essential to understanding the decentralized navigation algorithm discussed in future sections of this paper.

Figure 1 below depicts one possible tightly coupled GPS/INS integration algorithm for a stand-alone user who has access to dual frequency measurements.

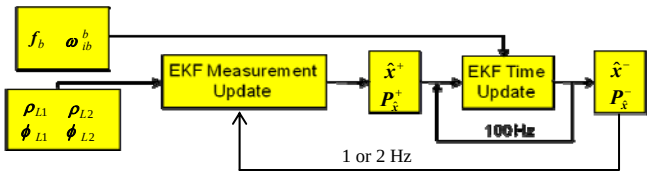

Figure 1: Stand-alone tightly coupled GPS/INS algorithm for a dual frequency user

In this algorithm, an extended Kalman filter (EKF) is used to accommodate the nonlinearities introduced by the INS dynamic models. Low rate GPS measurements of L1 and L2 code phase (ρ_{L1} and ρ_{L2}) and L1 and L2 carrier phase (ϕ_{L1} and ϕ_{L2}) are processed in the EKF measurement update to produce the current estimate of the state vector, $\hat{x}^+$ and it's associated covariance matrix, $P_{\hat{x}}^+$. During the time update, high rate inertial measurements of specific force (f_b) and inertial angular velocity ($^i\omega_b^b$) are processed at the raw output rate of the IMU, assumed here to be 100 Hz. The output of the time update is a high rate estimate of the state vector, $\hat{x}^-$ and it's associated covariance matrix, $P_{\hat{x}}^-$.

GPS MEASUREMENT MODELS

To determine the structure of the state vector first requires a measurement model for the code and carrier phase measurements. L1 and L2 code and carrier phase measurements are modeled as:

$$\rho_{L1}^i = \left\| x_{sv}^i - x_u \right\| + \delta t_u + \delta x_{clk-eph}^i + T^i + I_{L1}^i + m_{\rho,L1}^i + \nu_{\rho,L1}^i \quad (1)$$

$$\rho_{L2}^i = \left\| x_{sv}^i - x_u \right\| + \delta t_u + \delta x_{clk-eph}^i + T^i + \frac{f_{L1}^2}{f_{L2}^2} I_{L1}^i + m_{\rho,L2}^i + \nu_{\rho,L2}^i \quad (2)$$

$$\phi_{L1}^i = \left\| x_{sv}^i - x_u \right\| + \delta t_u + \delta x_{clk-eph}^i + \lambda_{L1} N_{L1}^i + T^i - I_{L1}^i + m_{\phi,L1}^i + \nu_{\phi,L1}^i \quad (3)$$

$$\phi_{L2}^i = \left\| x_{sv}^i - x_u \right\| + \delta t_u + \delta x_{clk-eph}^i + \lambda_{L2} N_{L2}^i + T^i - \frac{f_{L1}^2}{f_{L2}^2} I_{L1}^i + m_{\phi,L2}^i + \nu_{\phi,L2}^i \quad (4)$$

where x_{sv}^i is the ECEF position vector of satellite *i*, x_u is the ECEF position vector of the user, δt_u is the user clock bias expressed in meters, $\delta x_{clk-eph}^i$ is the combined satellite clock and ephemeris error for satellite *i* expressed in meters, λ_{L1} is the wavelength of the L1 carrier signal, λ_{L2} is the wavelength of the L2 carrier signal, N_{L1}^i is the L1 carrier phase cycle ambiguity for satellite *i*, N_{L2}^i is the L2 carrier phase cycle ambiguity, T^i is the residual tropospheric delay for satellite *i*, I_{L1}^i is the residual ionospheric delay on the L1 frequency for satellite *i*, f_{L1} is the frequency of the L1 carrier signal, f_{L2} is the

frequency of the L2 carrier signal, $m^i_{\rho,L1}$ is the L1 code phase multipath for satellite *i*, $m^i_{\rho,L2}$ is the L2 code phase multipath for satellite *i*, $m^i_{\phi,L1}$ is the L1 carrier phase multipath for satellite *i*, $m^i_{\phi,L2}$ is the L2 carrier phase multipath for satellite *i*, $v^i_{\rho,L1}$ is the thermal noise on the L1 code phase measurement from satellite *i*, $v^i_{\rho,L2}$ is the thermal noise on the L2 code phase measurement from satellite *i*, $v^i_{\phi,L1}$ is the thermal noise on the L1 carrier phase measurement and $v^i_{\phi,L2}$ is the thermal noise on the L2 carrier phase measurement. It is important to notice here that for the sake of simplification, the inter-frequency bias has not been included in the measurement models given in equations (1) through (4). The reason for this omission stems from the fact that this error will be canceled out in certain measurement linear combinations, discussed below.

For a user with access to dual frequency measurements, we can eliminate the ionospheric error by forming the following linear combinations of the code and carrier phase observables:

$$\rho^{\,i}_{IF} = \frac{f_{L1}^2}{f_{L1}^2 - f_{L2}^2}\rho^{\,i}_{L1} - \frac{f_{L2}^2}{f_{L1}^2 - f_{L2}^2}\rho^{\,i}_{L2} \tag{5}$$

$$\phi^{\,i}_{IF} = \frac{f_{L1}^2}{f_{L1}^2 - f_{L2}^2}\phi^{\,i}_{L1} - \frac{f_{L2}^2}{f_{L1}^2 - f_{L2}^2}\phi^{\,i}_{L2} \tag{6}$$

Applying these linear combinations to equations (1) through (4) yields the following iono-free code and carrier phase measurement models:

$$\begin{aligned}\rho^{\,i}_{IF} = {} & \left\|\boldsymbol{x}^i_{sv} - \boldsymbol{x}_u\right\| + \delta t_u + \delta x^{\,i}_{clk-eph} + \\ & T^i + m^i_{\rho,IF} + v^i_{\rho,IF}\end{aligned} \tag{7}$$

$$\begin{aligned}\phi^{\,i}_{IF} = {} & \left\|\boldsymbol{x}^i_{sv} - \boldsymbol{x}_u\right\| + \delta t_u + \delta x^{\,i}_{clk-eph} + N^i_{IF} + \\ & T^i + m^i_{\phi,IF} + v^i_{\phi,IF}\end{aligned} \tag{8}$$

It is important to notice here that although we have eliminated the ionospheric error, we have increased the thermal noise levels. In addition, we have lost the integer nature of the cycle ambiguities by performing the linear operation given in equation (6). That is, N^i_{IF} is no longer an integer, but instead is a floating point number.

The tightly coupled architecture shown in figure 1 can now be redrawn using iono-free GPS measurements instead of individual L1 and L2 code and carrier phase measurements.

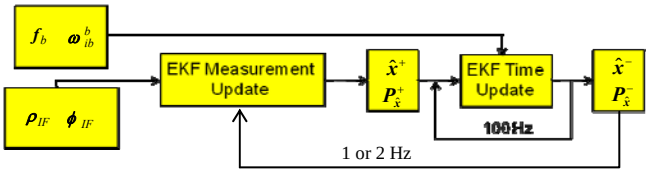

Figure 2: Stand-alone tightly coupled GPS/INS algorithm using iono-free GPS measurements

MEASUREMENT ERROR MODELS

The basic state variables in equations (7) and (8) are the ECEF user position vector, embedded in the vector norm, the receiver clock bias and the iono-free ambiguity state. However, there are a number of additional error sources shown in these equations. Proper modeling of these error sources is required to ensure that the state estimate and associated covariance matrix are meaningful. This section will describe the error models used in the Kalman filter.

SATELLITE CLOCK AND EPHEMERIS ERROR

It is well known that keeping precise time among satellites is critical to the success of GPS. Therefore high quality atomic standards are generally used onboard the satellites which exhibit low drift rates. In light of these observations, the satellite clock offset can be computed using the simple model:

$$\delta t^i_{sv} = a_0 + a_1(t - t_{oc}) + a_2(t - t_{oc})^2 \tag{9}$$

Where a_0, a_1 and a_2 are the satellite clock parameters broadcast in the navigation message, t_{oc} is the time-of-clock parameter broadcast in the ephemeris data message and t is the current time since t_{oc}. For the majority of GPS satellites, the quadratic coefficient a_2 is zero, suggesting that a linear model for the satellite clock error is adequate.

In contrast, GPS satellite ephemeris error shows a sinusoidal variation over a period of approximately 12 hours. An example of the cross track, radial and along track ephemeris error is shown below in figure 3 [10].

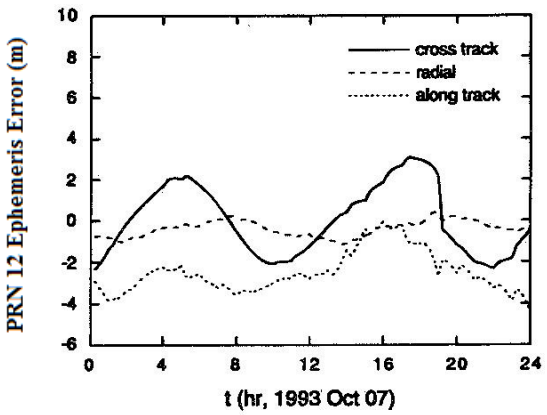

Figure 3: Ephemeris error components for PRN 12 [10].

In this work, we consider navigation applications with duration on the order of 1 hour. Over this period it is sufficient to model the satellite ephemeris error as a quadratic function with three unknown parameters. Combining the satellite clock and ephemeris errors together yields the error model:

$$\delta x^i_{clk-eph} = b^i_0 + b^i_1(t - t_{oc}) + b^i_2(t - t_{oc})^2 \qquad (10)$$

where b^i_0, b^i_1 and b^i_2 are three additional states per satellite that are estimated in the filter.

RESIDUAL TROPOSPHERIC ERROR

The stand-alone user has many models for the tropospheric delay at his/her disposal. A handful of possible models can be found in [12]. In this work, we adopt the model used in the LAAS program, which assumes that refractivity varies exponentially with height [4]. Under this assumption, the vertical tropospheric delay is governed by the equation:

$$T^i_{vert} = 10^{-6} N_s h_0 \left(e^{-h/h_0} - e^{-h_T/h_0} \right) \qquad (11)$$

Where N_s is the surface refractivity index, h_0 is the tropospheric scale height (taken to be 7000 m), h_T is the total height of the troposphere (taken to be 40000 m) and h is the current height of the user.

The surface refractivity cannot be known precisely, and will be in error by some small amount, δN_s. Therefore, an additional scalar state is added to the filter in order to model this small residual error.

In order to convert the vertical delay given in equation (11) into an actual slant delay, an obliquity factor must be applied, which is a function of the satellite elevation angle.

$$c^i_T = \frac{1}{\sqrt{0.002 + \sin^2 \theta_i}} \qquad (12)$$

Combining equations (11) and (12) yields the total tropospheric delay:

$$T^i = 10^{-6} N_s h_0 c^i_T \left(e^{-h/h_0} - e^{-h_T/h_0} \right) \qquad (13)$$

IONO-FREE MULTIPATH ERRORS

Both the iono-free code and carrier phase measurements are corrupted by multipath. This error source tends to be correlated in time and is a function of the surrounding environment. To account for the time correlated nature of multipath, state augmentation is used in the Kalman filter. Each satellite is given its own iono-free code and carrier phase multipath state which is modeled as a first order Gauss-Markov process. The dynamic behavior of these states is governed by the continuous differential equations:

$$\dot{m}^i_{\rho,IF} = -\frac{1}{\tau_{mp}} m^i_{\rho,IF} + w_{\rho,IF} \qquad (14)$$

$$\dot{m}^i_{\phi,IF} = -\frac{1}{\tau_{mp}} m^i_{\phi,IF} + w_{\phi,IF} \qquad (15)$$

Where τ_{mp} is the time constant of the process, $w_{\rho,IF}$ is the driving white noise for the iono-free code phase multipath state and $w_{\phi,IF}$ is the driving white noise for the iono-free carrier phase multipath state.

If we let n indicate the number of visible satellites, we will have 3 states for the user position (x, y and z), 1 state for the receiver clock bias, 3n states for the satellite clock and ephemeris error, 1 state for the residual tropospheric error, n states for the iono-free code phase multipath and n states for the iono-free carrier phase multipath.

GPS OBSERVATION MATRIX

The Kalman measurement update requires the measurements to be linearly related to the state variables, i.e.

$$\boldsymbol{z} = \boldsymbol{H}\,\boldsymbol{x} + \boldsymbol{v} \qquad (16)$$

Before we can write equations (7) and (8) in the form of equation (16), we must expand these equations using a first order Taylor series expansion.

$$\rho^{i}_{IF} \approx \left\| \boldsymbol{x}^{i}_{sv} - \boldsymbol{x}^{*}_{u} \right\| - \hat{\boldsymbol{e}}^{i} \cdot \left(\boldsymbol{x}_{u} - \boldsymbol{x}^{*}_{u} \right) + \delta t_{u} + \delta x^{i}_{clk-eph} + T^{i} + m^{i}_{\rho,IF} + \nu^{i}_{\rho,IF} \tag{17}$$

$$\phi^{i}_{IF} \approx \left\| \boldsymbol{x}^{i}_{sv} - \boldsymbol{x}^{*}_{u} \right\| - \hat{\boldsymbol{e}}^{i} \cdot \left(\boldsymbol{x}_{u} - \boldsymbol{x}^{*}_{u} \right) + \delta t_{u} + \delta x^{i}_{clk-eph} + N^{i}_{IF} + T^{i} + m^{i}_{\phi,IF} + \nu^{i}_{\phi,IF} \tag{18}$$

where $\hat{\boldsymbol{e}}^{i}$ is the line of sight unit vector originating at the user and terminating at the satellite and $\boldsymbol{x}^{*}_{u}$ is the best available estimate of the user's current ECEF position vector.

If we bring all known terms to the left hand side, equations (17) and (18) can be written as:

$$\rho^{i}_{IF} - \left\| \boldsymbol{x}^{i}_{sv} - \boldsymbol{x}^{*}_{u} \right\| - \hat{\boldsymbol{e}}^{i} \cdot \boldsymbol{x}^{*}_{u} = -\hat{\boldsymbol{e}}^{i} \cdot \boldsymbol{x}_{u} + \delta t_{u} + \delta x^{i}_{clk-eph} + T^{i} + m^{i}_{\rho,IF} + \nu^{i}_{\rho,IF} \tag{19}$$

$$\phi^{i}_{IF} - \left\| \boldsymbol{x}^{i}_{sv} - \boldsymbol{x}^{*}_{u} \right\| - \hat{\boldsymbol{e}}^{i} \cdot \boldsymbol{x}^{*}_{u} = -\hat{\boldsymbol{e}}^{i} \cdot \boldsymbol{x}_{u} + \delta t_{u} + \delta x^{i}_{clk-eph} + N^{i}_{IF} + T^{i} + m^{i}_{\phi,IF} + \nu^{i}_{\phi,IF} \tag{20}$$

If we make the following definitions:

$$\boldsymbol{x}_{G} = \begin{bmatrix} \boldsymbol{x}_{u} & \delta t_{r} & \delta \boldsymbol{x}_{ck-eph} & \boldsymbol{N}_{IF} & \delta N_{s} & \boldsymbol{m}_{\rho,IF} & \boldsymbol{m}_{\phi,IF} \end{bmatrix} \tag{21}$$

$$z^{i}_{\rho,IF} = \rho^{i}_{IF} - \left\| \boldsymbol{x}^{i}_{sv} - \boldsymbol{x}^{*}_{u} \right\| - \hat{\boldsymbol{e}}^{i} \cdot \boldsymbol{x}^{*}_{u} \tag{22}$$

$$z^{i}_{\phi,IF} = \phi^{i}_{IF} - \left\| \boldsymbol{x}^{i}_{sv} - \boldsymbol{x}^{*}_{u} \right\| - \hat{\boldsymbol{e}}^{i} \cdot \boldsymbol{x}^{*}_{u} \tag{23}$$

And stack all available measurements into one measurement vector, we get the measurement equation:

$$\begin{bmatrix} \boldsymbol{z}_{\rho,IF} \\ \boldsymbol{z}_{\phi,IF} \end{bmatrix} = \begin{bmatrix} \boldsymbol{H}_{\rho,IF} \\ \boldsymbol{H}_{\phi,IF} \end{bmatrix} \boldsymbol{x}_{G} + \begin{bmatrix} \boldsymbol{\nu}_{\rho,IF} \\ \boldsymbol{\nu}_{\phi,IF} \end{bmatrix} \tag{24}$$

Where:

$$\boldsymbol{H}_{\rho,IF} = \begin{bmatrix} \boldsymbol{G} & \mathbf{1} & \boldsymbol{H}_{clk-eph} & \mathbf{0} & \boldsymbol{H}_{T} & \boldsymbol{I} & \mathbf{0} \end{bmatrix} \tag{25}$$

$$\boldsymbol{H}_{\phi,IF} = \begin{bmatrix} \boldsymbol{G} & \mathbf{1} & \boldsymbol{H}_{clk-eph} & \boldsymbol{I} & \boldsymbol{H}_{T} & \mathbf{0} & \boldsymbol{I} \end{bmatrix} \tag{26}$$

and $\boldsymbol{G}$ is the geometry matrix containing the negative of the line of sight unit vectors to all visible satellites, $\mathbf{1}$ is a column vector of ones, $\boldsymbol{H}_{clk-eph}$ is a block diagonal matrix containing the coefficients in front of the b_k's in equation (10), $\boldsymbol{H}_{T}$ is a column vector containing the coefficient term in front of N_s in equation (13) for all visible satellites and $\boldsymbol{I}$ is an identity matrix.

Equation (24) is a linear measurement model relating the iono-free code and carrier phase measurements to the stand-alone GPS state vector given in equation (21). The next step is to bring in the inertial navigation information that will be used in the time update segment of the extended Kalman filter.

INS MECHANIZATION EQUATIONS

The derivation of the INS mechanization equations can be found in many textbooks devoted to the fundamental theory of inertial navigation, such as [6], [7] and [8]. Inertial measurement units (IMUs) use accelerometers and gyroscopes to determine a user's position and orientation in space. The equations of motion for these devices are derived from physics, and are stated below as equations (27) and (28).

$$\frac{{}^{n}d\,{}^{e}\boldsymbol{v}^{u}_{n}}{dt} = {}^{n}\boldsymbol{R}^{b}\,\boldsymbol{f}_{b} - \left(2\,{}^{i}\boldsymbol{\omega}^{e}_{n} + {}^{e}\boldsymbol{\omega}^{n}_{n} \right) \times {}^{e}\boldsymbol{v}^{u}_{n} + \boldsymbol{g}_{l} \tag{27}$$

$$\frac{d\boldsymbol{\zeta}}{dt} = \boldsymbol{F}_{eu} \left[{}^{i}\boldsymbol{\omega}^{b}_{b} - {}^{b}\boldsymbol{R}^{n} \left({}^{i}\boldsymbol{\omega}^{e}_{n} + {}^{e}\boldsymbol{\omega}^{n}_{n} \right) \right] \tag{28}$$

where ${}^{e}\boldsymbol{v}^{u}_{n}$ is the ground velocity of the user, ${}^{n}\boldsymbol{R}^{b}$ is the body-to-navigation rotation matrix for the user, $\boldsymbol{f}_{b}$ is the specific force measurement expressed in the user's body frame, ${}^{i}\boldsymbol{\omega}^{e}_{n}$ is the inertial angular velocity of the Earth, ${}^{e}\boldsymbol{\omega}^{n}_{n}$ is the angular velocity of the user's navigation frame relative to Earth, $\boldsymbol{g}_{l}$ is a model of the local gravity vector, $\boldsymbol{\zeta}$ is a vector containing the roll, pitch and yaw Euler angles of the user, $\boldsymbol{F}_{eu}$ is the matrix relating the rate of change of the Euler angles to the angular velocity of the body frame relative to the navigation frame and ${}^{i}\boldsymbol{\omega}^{b}_{b}$ is the inertial angular velocity measurement expressed in the user's body frame.

Before continuing, it is instructive to describe the vector notation given in equations (27) and (28). This nomenclature will be used in all further derivations provided in this paper.

As an example, consider the velocity term, ${}^{e}\boldsymbol{v}^{u}_{n}$. The upper right superscript, *u*, indicates that we are talking about the velocity of the user. The left superscript, *e*, is

used to indicate that this term is the velocity of the user relative to the earth. Finally, the right subscript, *n*, is used to inform the reader that this vector is expressed in the navigation frame attached to the user.

To illustrate this convention again, consider the gyroscope measurement, ${}^{i}\boldsymbol{\omega}_{b}^{b}$. This term represents the inertial angular velocity of the body frame (upper right superscript) relative to inertial space (upper left superscript) expressed in the body frame attached to the user (lower right subscript).

Specific quantities given in equations (27) and (28) are defined as:

$$ {}^{i}\boldsymbol{\omega}_{n}^{e} = \begin{bmatrix} \Omega_e \cos L & 0 & -\Omega_e \sin L \end{bmatrix}^T \tag{29} $$

$$ {}^{e}\boldsymbol{\omega}_{n}^{n} = \begin{bmatrix} \dfrac{{}^{e}v_{e}^{u}}{r_p + h} & -\dfrac{{}^{e}v_{n}^{u}}{r_m + h} & -\dfrac{{}^{e}v_{e}^{u} \tan L}{r_p + h} \end{bmatrix}^T \tag{30} $$

$$ \boldsymbol{F}_{eu} = \begin{bmatrix} 1 & \tan\theta \sin\phi & \tan\theta \cos\phi \\ 0 & \cos\phi & -\sin\phi \\ 0 & \sin\phi \sec\theta & \cos\phi \sec\theta \end{bmatrix} \tag{31} $$

Where Ω_e is the rotation rate of the Earth, L is the latitude of the user, ${}^{e}v_{n}^{u}$ is the north component of the user's ground velocity, ${}^{e}v_{e}^{u}$ is the east component of the user's ground velocity, r_p is the prime radius of curvature, r_m is the meridian radius of curvature and h is the height of the user.

Given the definitions in equations (29) through (31), it is obvious that equations (27) and (28) define a set of coupled, non-linear differential equations. Before these equations can be used in the EKF, they must be linearized with respect to the state variables. Using a very general notation, we can write equations (27) and (28) in the form:

$$ \frac{{}^{n}d\,{}^{e}\boldsymbol{v}^{u}}{dt} = \boldsymbol{q}_v(\boldsymbol{x}_{u,g}\ ,\ {}^{e}\boldsymbol{v}^{u}\ ,\ \boldsymbol{\zeta}\ ,\ \boldsymbol{f}_b) \tag{32} $$

$$ \frac{d\boldsymbol{\zeta}}{dt} = \boldsymbol{q}_\zeta(\boldsymbol{x}_{u,g}\ ,\ {}^{e}\boldsymbol{v}^{u}\ ,\ \boldsymbol{\zeta}\ ,\ \boldsymbol{\omega}_{ib}^{b}) \tag{33} $$

where $\boldsymbol{q}_v$ denotes the non-linear function on the right hand side of equation (27), $\boldsymbol{q}_\zeta$ denotes the non-linear function on the right hand side of equation (28) and $\boldsymbol{x}_{u,g}$ denotes the geodetic coordinates of the user (latitude, longitude and height).

Equations (32) and (33) can now be expanded in a Taylor series about the current state estimate to produce linearized dynamic models suitable for use in a Kalman filter.

$$ \frac{{}^{n}d\,\delta\,{}^{e}\boldsymbol{v}_{n}^{u}}{dt} \approx \boldsymbol{F}_{vv}\,\delta\,{}^{e}\boldsymbol{v}_{n}^{u} + \boldsymbol{F}_{vx}\,\delta\,\boldsymbol{x}_{u,g} + \boldsymbol{F}_{v\zeta}\delta\boldsymbol{\zeta} + \boldsymbol{F}_{vf}\delta\,\boldsymbol{f}_b \tag{34} $$

$$ \frac{d\,\delta\boldsymbol{\zeta}}{dt} \approx \boldsymbol{F}_{\zeta v}\,\delta\,{}^{e}\boldsymbol{v}_{n}^{u} + \boldsymbol{F}_{\zeta x}\,\delta\,\boldsymbol{x}_{u,g} + \boldsymbol{F}_{\zeta\zeta}\delta\boldsymbol{\zeta} + \boldsymbol{F}_{\zeta\omega}\delta\,{}^{i}\boldsymbol{\omega}_{b}^{b} \tag{35} $$

The specific form of the coefficient $\boldsymbol{F}$ matrices in equations (34) and (35) can be found in [6]. Rather than using the Euler angle error vector, $\delta\boldsymbol{\zeta}$ it is customary to use an error vector, $\delta\boldsymbol{\mu}$, which describes the error in the body-to-navigation rotation matrix. These two error representations are related by the equation:

$$ \delta\boldsymbol{\mu} = \begin{bmatrix} \cos\psi\ \cos\theta & -\sin\psi & 0 \\ \sin\psi\ \cos\theta & \cos\psi & 0 \\ -\sin\theta & 0 & 1 \end{bmatrix} \delta\boldsymbol{\zeta} \tag{36} $$

Applying this transformation equation to equations (34) and (35) yields the two error differential equations:

$$ \frac{{}^{n}d\,\delta\,{}^{e}\boldsymbol{v}_{n}^{u}}{dt} \approx \boldsymbol{F}_{vv}\,\delta\,{}^{e}\boldsymbol{v}_{n}^{u} + \boldsymbol{F}_{vx}\,\delta\,\boldsymbol{x}_{u,g} + \boldsymbol{F}_{v\mu}\delta\,\boldsymbol{\mu} + \boldsymbol{F}_{vf}\delta\,\boldsymbol{f}_b \tag{37} $$

$$ \frac{d\,\delta\,\boldsymbol{\mu}}{dt} \approx \boldsymbol{F}_{\mu v}\,\delta\,{}^{e}\boldsymbol{v}_{n}^{u} + \boldsymbol{F}_{\mu x}\,\delta\,\boldsymbol{x}_{u,g} + \boldsymbol{F}_{\mu\mu}\delta\,\boldsymbol{\mu} + \boldsymbol{F}_{\mu\omega}\delta\,{}^{i}\boldsymbol{\omega}_{b}^{b} \tag{38} $$

Notice in these two equations that we have linearized the INS mechanization equations with respect to the geodetic coordinates of the user. However, the GPS position state in equation (21) is an ECEF position state. It is possible to relate the geodetic position error to the ECEF position error by performing a Taylor series expansion on the following equations:

$$ \begin{bmatrix} x \\ y \\ z \end{bmatrix} = \begin{bmatrix} (r_p + h)\cos L \cos\lambda \\ (r_p + h)\cos L \sin\lambda \\ (r_p(1 - e^2) + h)\sin L \end{bmatrix} \tag{39} $$

yielding:

$$ \delta\,\boldsymbol{x}_u = \boldsymbol{F}_u\,\delta\,\boldsymbol{x}_{u,g} \tag{40} $$

Equation (40) can be substituted into equations (37) and (38) to retain a position state in ECEF coordinates.

The final two terms that need to be addressed in equations (37) and (38) are the inertial measurement errors, $\delta\,\boldsymbol{f}_b$

and $\delta\,{}^{i}\boldsymbol{\omega}_{b}^{b}$. These error sources are modeled in this work as the sum of white measurement noise and a time-varying bias. That is:

$$\begin{aligned}\delta\,\boldsymbol{f}_b &= \boldsymbol{\nu}_a + \boldsymbol{b}_a \\ \delta\,{}^{i}\boldsymbol{\omega}_{b}^{b} &= \boldsymbol{\nu}_g + \boldsymbol{b}_g\end{aligned} \tag{41}$$

where $\boldsymbol{\nu}_a$ is a white measurement noise vector on the accelerometer, $\boldsymbol{\nu}_g$ is a white measurement noise vector on the gyroscope, $\boldsymbol{b}_a$ is the accelerometer bias and $\boldsymbol{b}_g$ is the gyroscope bias.

The accelerometer bias and gyroscope bias are both modeled as 1st order Gauss-Markov processes and estimated as additional states in the EKF. The dynamic models for these states are given by:

$$\begin{aligned}\dot{\boldsymbol{b}}_a &= -\frac{1}{\tau_a}\boldsymbol{b}_a + \boldsymbol{w}_a \\ \dot{\boldsymbol{b}}_g &= -\frac{1}{\tau_g}\boldsymbol{b}_g + \boldsymbol{w}_g\end{aligned} \tag{42}$$

where τ_a is the time constant of the accelerometer bias, τ_g is the time constant of the gyroscope bias, $\boldsymbol{w}_a$ is the driving white noise for the accelerometer bias state and $\boldsymbol{w}_g$ is the driving white noise for the gyroscope bias state.

For the inertial navigation system, the state vector consists of the velocity state, body-to-navigation rotation matrix error state, accelerometer bias state and gyroscope bias state.

$$\boldsymbol{x}_I = \begin{bmatrix} {}^{e}\boldsymbol{v}_n^u & \delta\boldsymbol{\mu} & \boldsymbol{b}_a & \boldsymbol{b}_g \end{bmatrix} \tag{43}$$

Our goal is to define a linearized dynamic model for the GPS state vector given in equation (21) and the INS state vector given in equation (43). The linearized dynamic model for the INS state vector and the ECEF position state is given by:

$$\begin{bmatrix} \delta\,{}^{e}\dot{\boldsymbol{v}}_n^u \\ \delta\dot{\boldsymbol{\mu}} \\ \dot{\boldsymbol{b}}_a \\ \dot{\boldsymbol{b}}_g \\ \delta\dot{\boldsymbol{x}}_u \end{bmatrix} = \begin{bmatrix} \boldsymbol{F}_{vv} & \boldsymbol{F}_{v\mu} & \boldsymbol{F}_{vf} & \boldsymbol{0} & \boldsymbol{F}_{vx} \\ \boldsymbol{F}_{\mu v} & \boldsymbol{F}_{\mu\mu} & \boldsymbol{0} & \boldsymbol{F}_{\mu\omega} & \boldsymbol{F}_{\mu x} \\ \boldsymbol{0} & \boldsymbol{0} & -\boldsymbol{I}/\tau_a & \boldsymbol{0} & \boldsymbol{0} \\ \boldsymbol{0} & \boldsymbol{0} & \boldsymbol{0} & -\boldsymbol{I}/\tau_g & \boldsymbol{0} \\ \boldsymbol{F}_{xv} & \boldsymbol{0} & \boldsymbol{0} & \boldsymbol{0} & \boldsymbol{F}_{xx} \end{bmatrix} \begin{bmatrix} \delta\,{}^{e}\boldsymbol{v}^u \\ \delta\boldsymbol{\mu} \\ \boldsymbol{b}_a \\ \boldsymbol{b}_g \\ \delta\boldsymbol{x}_u \end{bmatrix} + \begin{bmatrix} \boldsymbol{F}_{vf}\boldsymbol{\nu}_a \\ \boldsymbol{F}_{\mu\omega}\boldsymbol{\nu}_g \\ \boldsymbol{w}_a \\ \boldsymbol{w}_g \\ \boldsymbol{0} \end{bmatrix} \tag{44}$$

The last step in completely specifying the EKF for the stand-alone user is to specify the dynamic model for the state vector $\boldsymbol{x}_G$ given in equation (21). We exclude the ECEF position state because its dynamic model has already been specified in equation (44).

$$\begin{bmatrix} \delta\dot{t}_r \\ \delta\dot{\boldsymbol{x}}_{clk-eph} \\ \dot{\boldsymbol{N}}_{IF} \\ \delta\dot{N}_s \\ \dot{\boldsymbol{m}}_{\rho,IF} \\ \dot{\boldsymbol{m}}_{\phi,IF} \end{bmatrix} = \begin{bmatrix} 0 & \boldsymbol{0} & \boldsymbol{0} & 0 & \boldsymbol{0} & \boldsymbol{0} \\ \boldsymbol{0} & \boldsymbol{0} & \boldsymbol{0} & \boldsymbol{0} & \boldsymbol{0} & \boldsymbol{0} \\ \boldsymbol{0} & \boldsymbol{0} & \boldsymbol{0} & \boldsymbol{0} & \boldsymbol{0} & \boldsymbol{0} \\ 0 & \boldsymbol{0} & \boldsymbol{0} & 0 & \boldsymbol{0} & \boldsymbol{0} \\ \boldsymbol{0} & \boldsymbol{0} & \boldsymbol{0} & \boldsymbol{0} & -\boldsymbol{I}/\tau_m & \boldsymbol{0} \\ \boldsymbol{0} & \boldsymbol{0} & \boldsymbol{0} & \boldsymbol{0} & \boldsymbol{0} & -\boldsymbol{I}/\tau_m \end{bmatrix} \begin{bmatrix} \delta t_r \\ \delta\boldsymbol{x}_{clk-eph} \\ \boldsymbol{N}_{IF} \\ \delta N_s \\ \boldsymbol{m}_{\rho,IF} \\ \boldsymbol{m}_{\phi,IF} \end{bmatrix} + \begin{bmatrix} \infty \\ \boldsymbol{0} \\ \boldsymbol{0} \\ 0 \\ \boldsymbol{w}_{\rho,IF} \\ \boldsymbol{w}_{\phi,IF} \end{bmatrix} \tag{45}$$

The reader should notice that there is infinite process noise on the receiver clock state. This is done to let the filter know that we do not have an accurate dynamic model is place for the receiver clock.

Equations (44) and (45) can be written in a compact form as:

$$\delta\dot{\boldsymbol{x}} = \boldsymbol{F}\,\delta\boldsymbol{x} + \boldsymbol{\eta} \tag{46}$$

It is important to note that equation (46) is used only for covariance propagation in the EKF. The actual state

vector is propagated according to the non-linear dynamic models during the time update of the EKF. We therefore have a complete description of the EKF for the stand-alone user. This algorithm will be used again in the development of the decentralized filtering scheme discussed further below.

BASELINE DIFFERENTIAL GPS/INS NAVIGATION ALGORITHM

Let's turn our attention now to the problem of estimating the relative position vector between two users, defined as:

$$\Delta \boldsymbol{x} = \boldsymbol{x}_r - \boldsymbol{x}_u \tag{47}$$

Where $\boldsymbol{x}_r$ indicates the ECEF position vector of the reference station and $\Delta \boldsymbol{x}$ is the relative position vector in ECEF coordinates. If we differentiate both sides of equation (47) with respect to time in the ECEF frame, we arrive at the equation:

$$\frac{{}^e d\,\Delta \boldsymbol{x}}{dt} = {}^e\boldsymbol{v}^r - {}^e\boldsymbol{v}^u \tag{48}$$

Because equation (48) is a linear equation, the dynamic model for the relative position error obeys the exact same equation. That is:

$$\frac{{}^e d\,\delta\Delta \boldsymbol{x}}{dt} = \delta\,{}^e\boldsymbol{v}^r - \delta\,{}^e\boldsymbol{v}^u \tag{49}$$

where:

$$\delta\Delta \boldsymbol{x} = \delta \boldsymbol{x}_r - \delta \boldsymbol{x}_u \tag{50}$$

A very fortunate simplification occurs when the reference station is stationary. In this case, an accurate survey of the reference station can be made, rendering any residual error in the reference station's position negligible. Furthermore, the reference station velocity is zero, and hence its velocity error is zero. These two observations simplify equations (49) and (50) to:

$$\frac{{}^e d\,\delta\Delta \boldsymbol{x}}{dt} = \delta\,{}^e\boldsymbol{v}^r - \delta\,{}^e\boldsymbol{v}^u = -\delta\,{}^e\boldsymbol{v}^u \tag{51}$$

$$\delta\Delta \boldsymbol{x} = \delta \boldsymbol{x}_r - \delta \boldsymbol{x}_u \approx -\delta \boldsymbol{x}_u \tag{52}$$

However, for a mobile reference station, we cannot neglect the error in its position and velocity, and these quantities must be estimated along with the relative position vector. Ground velocity estimation requires the reference station to broadcast its raw inertial measurements to the user platform. If the reference station is undergoing high dynamic maneuvers, these measurements must be broadcast at a high data rate. Assuming that this is hypothetically possible, we can design the baseline differential GPS/INS algorithm shown in figure 4.

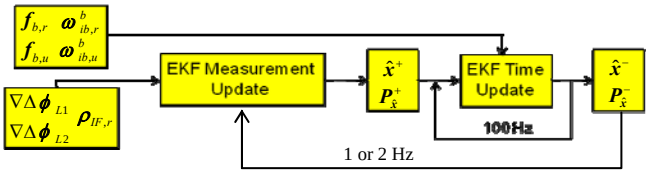

Figure 4: Baseline differential GPS/INS architecture

Notice that the estimation problem is still nonlinear, requiring us to use an EKF. The external aiding measurements from the GPS include double difference L1 and L2 carrier phase measurements ($\nabla\Delta\boldsymbol{\phi}_{L1}$ and $\nabla\Delta\boldsymbol{\phi}_{L2}$) and the ionosphere-free pseudorange measurement ($\boldsymbol{\rho}_{IF,r}$) broadcast from the reference platform. These measurements are different than those used in the stand-alone GPS/INS algorithm shown in figure 2. We are no longer using ionosphere-free carrier phase measurements in the measurement update. The reason for this pertains to the accuracy which is attainable in estimating the relative position vector. The iono-free linear combination introduces two adverse effects. First, the iono-free linear combination amplifies the measurement noise by approximately three, which will ultimately affect the accuracy of the estimated relative position vector. Secondly, recall that the iono-free linear combination causes us to lose the integer nature of the cycle ambiguities. This eliminates the possibility of performing cycle ambiguity resolution, which also results in degraded accuracy. Hence, we use the double difference carrier phase measurements instead to gain the maximum possible accuracy possible. However, we do still use the ionosphere-free pseudorange measurement from the reference platform to estimate its absolute position and velocity.

The double difference carrier phase measurements are formed by first differencing measurements between the user and reference station. This process eliminates the satellite clock and ephemeris errors. Then, these subsequent measurements are differenced again relative to a master satellite, eliminating the receiver clock bias. Hence, we obtain the following measurement models:

$$\begin{aligned}\nabla\Delta\phi^{i,j}_{L1} &= -\left(\hat{\boldsymbol{e}}^i - \hat{\boldsymbol{e}}^j\right)\cdot\Delta\boldsymbol{x} + \lambda_{L1}\nabla\Delta N^{ij}_{L1} + \\ &\left(\Delta m^i_{\phi,L1} - \Delta m^j_{\phi,L1}\right) + \delta T^{ij} + \delta I^{ij} + \nu^{ij}_{\nabla\Delta\phi,L1}\end{aligned} \tag{52}$$

$$\nabla\Delta\phi_{L2}^{i,j} = -\left(\hat{\boldsymbol{e}}^{i} - \hat{\boldsymbol{e}}^{j}\right)\cdot\Delta\boldsymbol{x} + \lambda_{L2}\nabla\Delta N_{L2}^{ij} + \left(\Delta m_{\phi,L2}^{i} - \Delta m_{\phi,L2}^{j}\right) + \delta T^{ij} + \frac{f_{L1}^2}{f_{L2}^2}\delta I^{ij} + \nu_{\nabla\Delta\phi,L2}^{ij} \quad (53)$$

where $\nabla\Delta N_{L1}^{ij}$ and $\nabla\Delta N_{L2}^{ij}$ are the double difference L1 and L2 cycle ambiguities for satellites *i* and *j*, respectively, $\Delta m_{\phi,L1}^{i}$ and $\Delta m_{\phi,L2}^{i}$ are the L1 and L2 single difference carrier phase multipath errors for satellite *i*, respectively, δT^{ij} is the residual tropospheric error, δI^{ij} is the residual ionospheric error on the L1 frequency and $\nu_{\nabla\Delta\phi,L1}^{ij}$ and $\nu_{\nabla\Delta\phi,L2}^{ij}$ are the double difference carrier phase measurement noise on L1 and L2, respectively.

In this algorithm, L1 and L2 single difference multipath states are modeled as 1st order Gauss-Markov processes. In order to model the spatial decorrelation errors for the troposphere and ionosphere, the LAAS accuracy models from [4] are employed.

From [4], the residual tropospheric decorrelation error can be modeled as:

$$\delta T^{i} = 10^{-6} c_T^{i} N_s h_0 \left(1 - e^{-\Delta h / h_0}\right) \quad (54)$$

where δT^{i} is the residual tropospheric error after differencing measurements between the user and reference station for satellite *i* and Δh is the height of the user above the reference station.

A similar approach can be taken to model the residual ionospheric error. In this case, the residual vertical error is modeled as [4]:

$$\delta I_{vert}^{i} = c_I^{i}\left(\Delta n \cdot g_{vi,n}^{i} + \Delta e \cdot g_{vi,e}^{i}\right) \quad (55)$$

Where Δn is the separation between the user and reference station in the north direction, Δe is the separation between the user and reference station in the east direction, $g_{vi,n}^{i}$ is the vertical ionospheric gradient in the north direction for satellite *i*, $g_{vi,e}^{i}$ is the vertical ionospheric gradient in the east direction for satellite *i* and c_I^{i} is an obliquity factor, defined as:

$$c_I^{i} = \left[1 - \left(\frac{R_e \cos\theta_i}{R_e + h_I}\right)^2\right]^{-1/2} \quad (56)$$

The resulting GPS state vector for relative positioning is described by:

$$\boldsymbol{x}_{G,ur} = \left[\Delta\boldsymbol{x} \;\; \nabla\Delta\boldsymbol{N}_{L1} \;\; \nabla\Delta\boldsymbol{N}_{L2} \;\; \Delta\boldsymbol{m}_{\phi,L1} \;\; \Delta\boldsymbol{m}_{\phi,L2} \;\; \delta N_s \;\; \boldsymbol{g}_{vi,n} \;\; \boldsymbol{g}_{vi,e}\right]^T \quad (57)$$

In addition, we must add the following three additional state vectors to the estimation problem:

$$\boldsymbol{x}_{I,r} = \left[{}^{e}\boldsymbol{v}^{r} \quad \delta\boldsymbol{\mu}_r \quad \boldsymbol{b}_{a,r} \quad \boldsymbol{b}_{g,r}\right] \quad (58)$$

$$\boldsymbol{x}_{I,u} = \left[{}^{e}\boldsymbol{v}^{u} \quad \delta\boldsymbol{\mu}_u \quad \boldsymbol{b}_{a,u} \quad \boldsymbol{b}_{g,u}\right] \quad (59)$$

$$\boldsymbol{x}_{G,IF} = \left[\boldsymbol{x}_r \quad \delta t_r \quad \delta\boldsymbol{x}_{ck-eph} \quad \boldsymbol{m}_{\rho,IF}\right] \quad (60)$$

The linearized dynamic model for equations (58) and (60) has already been specified in equations (44) and (45). Equation (59) has a linearized dynamic model completely analogous to equation (44) except that the position error state is absent. This state is replaced by the dynamic model for the relative position vector error state given in equation (49).

For the remaining states given in equation (57), the dynamic models are trivial. The double difference cycle ambiguity states are constant, so their time rate of change is zero. In addition, the ionospheric gradient terms are assumed to be constant over the course of the navigation operation. The single difference L1 and L2 carrier phase multipath states are modeled using a 1st order Gauss-Markov process.

Hence, we have a complete state-space formulation that can be used in an EKF algorithm to estimate the relative position vector between the reference station and the user.

DECENTRALIZED NAVIGATION ALGORITHM

In many real life navigation applications, it will not be possible to broadcast 100 Hz raw inertial navigation data from the reference vehicle to the user platform. One possible alternative is to simply broadcast the raw inertial data at a lower rate, perhaps around 20 Hz. However, if the reference station is exhibiting highly dynamic behavior, 20 Hz measurements may not be sufficient to capture the motion. For example, consider an aircraft executing a rolling maneuver. Processing gyroscope measurements at 20 Hz will not be sufficient to estimate the Euler angles accurately. This is turn will result in an incorrect body-to-navigation rotation matrix which adversely affects position and velocity estimation.

In this work, we suppose that both the reference station and user are operating their own stand-alone, tightly coupled GPS/INS Kalman filter algorithms to produce

estimates of position, velocity and attitude (PVA). The reference station broadcasts these state estimates at a low data rate to a differential Kalman filter onboard the user platform, which together with the corresponding user-generated state estimates, constructs nominal values of the relative position and relative velocity states. Based on this nominal state trajectory, the filter then incorporates low rate-GPS differential code and carrier phase measurements to estimate the deviation of the true state from the nominal state. The situation is shown schematically in figure 5.

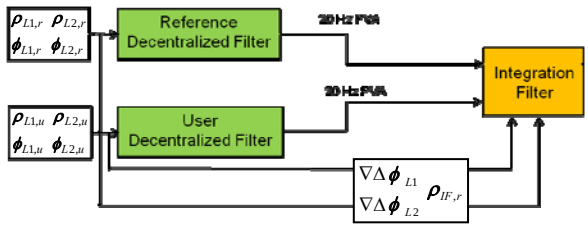

Figure 5: Decentralized GPS/INS algorithm

For the time being, let's focus on the states related to the inertial navigation systems.

At the reference vehicle and the user, we still must retain the INS state vectors given in equations (58) and (59). They are restated below as equations (61) and (62) for convenience.

$$\boldsymbol{x}_{I,r} = \begin{bmatrix} {}^{e}\boldsymbol{v}_n^r & \delta\boldsymbol{\mu}_r & \boldsymbol{b}_{a,r} & \boldsymbol{b}_{g,r} \end{bmatrix} \tag{61}$$

$$\boldsymbol{x}_{I,u} = \begin{bmatrix} {}^{e}\boldsymbol{v}_n^u & \delta\boldsymbol{\mu}_u & \boldsymbol{b}_{a,u} & \boldsymbol{b}_{g,u} \end{bmatrix} \tag{62}$$

In addition, we must also retain the GPS state vectors given in equations (57) and (60). These equations are restated below as equations (63) and (64).

$$\boldsymbol{x}_{G,ur} = \begin{bmatrix} \Delta\boldsymbol{x} & \nabla\Delta\boldsymbol{N}_{L1} & \nabla\Delta\boldsymbol{N}_{L2} & \Delta\boldsymbol{m}_{\phi,L1} & \Delta\boldsymbol{m}_{\phi,L2} & \delta N_S & \boldsymbol{g}_{vi,n} & \boldsymbol{g}_{vi,e} \end{bmatrix}^T \tag{63}$$

$$\boldsymbol{x}_{G,IF} = \begin{bmatrix} \boldsymbol{x}_r & \delta t_r & \delta\boldsymbol{x}_{ck-eph} & \boldsymbol{m}_{\rho,IF} \end{bmatrix} \tag{64}$$

The reason that we must retain these two GPS state vectors is because the decentralized GPS/INS filter is using the same measurements as the baseline differential GPS/INS algorithm. That is, we will still be using the double difference carrier phase measurements to estimate the relative position vector and the iono-free pseudorange observable from the reference platform to estimate its position and velocity.

We have already derived dynamic models for the INS state vectors given in equations (61) and (62). However, we are not interested in estimating the absolute position and velocity of the reference station and user. We are interested in estimating relative position and velocity. We can derive the dynamic model for the relative velocity by recalling the acceleration equation in the presence of rotating reference frames [13]:

$$\begin{aligned} {}^{e}\boldsymbol{a}^u = {}^{e}\boldsymbol{a}^r + {}^{r}\boldsymbol{a}^u + 2{}^{e}\boldsymbol{\omega}^{n_r} \times {}^{r}\boldsymbol{v}^u + {}^{e}\boldsymbol{\alpha}^{n_r} \times \Delta\boldsymbol{\chi} + \\ {}^{e}\boldsymbol{\omega}^{n_r} \times \left({}^{e}\boldsymbol{\omega}^{n_r} \times \Delta\boldsymbol{\chi} \right) \end{aligned} \tag{65}$$

where ${}^{e}\boldsymbol{a}^u$ is the ground acceleration of the user, ${}^{r}\boldsymbol{a}^u$ is the acceleration of the user relative to the reference station, ${}^{e}\boldsymbol{\omega}^{n_r}$ is the angular velocity of the reference station's navigation frame relative to Earth, ${}^{r}\boldsymbol{v}^u$ is the velocity of the user relative to the reference station, ${}^{e}\boldsymbol{\alpha}^{n_r}$ is the angular velocity of the reference station's navigation frame relative to Earth and $\Delta\boldsymbol{\chi}$ is the relative position vector originating at the reference station and terminating at the user.

To be consistent with the definition of the relative position vector given in equation (47), we make the following substitution:

$$\Delta\boldsymbol{\chi} = -\Delta\boldsymbol{x} \tag{66}$$

Furthermore, notice that:

$${}^{e}\boldsymbol{a}^u = {}^{n_u}\boldsymbol{R}^{b_u} \boldsymbol{f}_{b,u} - 2{}^{i}\boldsymbol{\omega}^{e} \times {}^{e}\boldsymbol{v}^u + \boldsymbol{g}_{l,u} \tag{67}$$

$${}^{e}\boldsymbol{a}^r = {}^{n_r}\boldsymbol{R}^{b_r} \boldsymbol{f}_{b,r} - 2{}^{i}\boldsymbol{\omega}^{e} \times {}^{e}\boldsymbol{v}^r + \boldsymbol{g}_{l,r} \tag{68}$$

$${}^{r}\boldsymbol{a}^u = \frac{{}^{n_r}d\,{}^{r}\boldsymbol{v}^u}{dt} \tag{69}$$

Substituting equations (66) through (69) into equation (65) yields:

$$\begin{aligned} \frac{{}^{n_r}d\,{}^{r}\boldsymbol{v}^u}{dt} = {}^{n_u}\boldsymbol{R}^{b_u} \boldsymbol{f}_{b,u} - 2{}^{i}\boldsymbol{\omega}^{e} \times {}^{e}\boldsymbol{v}^u + \boldsymbol{g}_{l,u} - \\ {}^{n_r}\boldsymbol{R}^{b_r} \boldsymbol{f}_{b,r} + 2{}^{i}\boldsymbol{\omega}^{e} \times {}^{e}\boldsymbol{v}^r - \boldsymbol{g}_{l,r} - \\ 2\,{}^{e}\boldsymbol{\omega}^{n_r} \times {}^{r}\boldsymbol{v}^u + {}^{e}\boldsymbol{\alpha}^{n_r} \times \Delta\boldsymbol{x} + \\ {}^{e}\boldsymbol{\omega}^{n_r} \times \left({}^{e}\boldsymbol{\omega}^{n_r} \times \Delta\boldsymbol{x} \right) \end{aligned} \tag{70}$$

But we know that:

$${}^{e}\boldsymbol{v}^u = {}^{e}\boldsymbol{v}^r + {}^{r}\boldsymbol{v}^u - {}^{e}\boldsymbol{\omega}^{n_r} \times \Delta\boldsymbol{x} \tag{71}$$

Substituting equation (71) into equation (70) gives the dynamic model for the relative velocity state:

$$\frac{{}^{n_r}d\,{}^{r}\boldsymbol{v}^{u}}{dt} = {}^{n_u}\boldsymbol{R}^{b_u}\boldsymbol{f}_{b,u} + \boldsymbol{g}_{l,u} - {}^{n_r}\boldsymbol{R}^{b_r}\boldsymbol{f}_{b,r} - \boldsymbol{g}_{l,r} + {}^{e}\boldsymbol{\alpha}^{n_r}\times\Delta\boldsymbol{x} + {}^{e}\boldsymbol{\omega}^{n_r}\times\left({}^{e}\boldsymbol{\omega}^{n_r}\times\Delta\boldsymbol{x}\right) - 2\,{}^{e}\boldsymbol{\omega}^{n_r}\times{}^{r}\boldsymbol{v}^{u} - 2\,{}^{i}\boldsymbol{\omega}^{e}\times\left({}^{r}\boldsymbol{v}^{u} - {}^{e}\boldsymbol{\omega}^{n_r}\times\Delta\boldsymbol{x}\right) \tag{72}$$

A recurring theme of this paper is the derivation of a dynamic model, followed by a Taylor series expansion for linearization. There is no exception here. If we expand equation (72) in a Taylor series, we can notice that every element of the state vector given in equation (61) will be present. However, we no longer have any states related to the absolute position and velocity of the user. Instead, what we have are relative position and velocity states. Therefore, the two inertial state vectors in the decentralized filter are given by:

$$\boldsymbol{x}_{I,r} = \begin{bmatrix}\delta\,{}^{e}\boldsymbol{v}_n^{r} & \delta\boldsymbol{\mu}_r & \boldsymbol{b}_{a,r} & \boldsymbol{b}_{g,r} & \delta\boldsymbol{x}_r\end{bmatrix} \tag{73}$$

$$\boldsymbol{x}_{I,u} = \begin{bmatrix}\delta\,{}^{r}\boldsymbol{v}_n^{u} & \delta\boldsymbol{\mu}_u & \boldsymbol{b}_{a,u} & \boldsymbol{b}_{g,u} & \delta\Delta\boldsymbol{x}\end{bmatrix} \tag{74}$$

The dynamic model for the state vector in equation (73) has already been given as equation (44) where a *u* is replaced by *r* to indicate that it is a dynamic model for the reference platform. The dynamic model for the state vector in equation (74) can be written as:

$$\begin{bmatrix}\delta\,{}^{r}\dot{\boldsymbol{v}}_n^{u}\\ \delta\dot{\boldsymbol{\mu}}_u\\ \dot{\boldsymbol{b}}_{a,u}\\ \dot{\boldsymbol{b}}_{g,u}\\ \delta\Delta\dot{\boldsymbol{x}}\end{bmatrix} = \begin{bmatrix}\boldsymbol{J}_{vv} & \boldsymbol{J}_{v\mu} & \boldsymbol{J}_{vf_u} & \boldsymbol{0} & \boldsymbol{J}_{vx}\\ \boldsymbol{J}_{\mu v} & \boldsymbol{J}_{\mu\mu} & \boldsymbol{0} & \boldsymbol{J}_{\mu\omega} & \boldsymbol{J}_{\mu x}\\ \boldsymbol{0} & \boldsymbol{0} & -\boldsymbol{I}/\tau_a & \boldsymbol{0} & \boldsymbol{0}\\ \boldsymbol{0} & \boldsymbol{0} & \boldsymbol{0} & -\boldsymbol{I}/\tau_g & \boldsymbol{0}\\ \boldsymbol{J}_{xv} & \boldsymbol{0} & \boldsymbol{0} & \boldsymbol{0} & \boldsymbol{J}_{xx}\end{bmatrix}\begin{bmatrix}\delta\,{}^{r}\boldsymbol{v}_n^{u}\\ \delta\boldsymbol{\mu}_u\\ \boldsymbol{b}_{a,u}\\ \boldsymbol{b}_{g,u}\\ \delta\Delta\boldsymbol{x}\end{bmatrix} + \begin{bmatrix}\boldsymbol{J}_{vf_u}\boldsymbol{\nu}_{a,u} + \boldsymbol{J}_{vf_r}\boldsymbol{\nu}_{a,r}\\ \boldsymbol{J}_{\mu\omega}\boldsymbol{\nu}_g\\ \boldsymbol{w}_a\\ \boldsymbol{w}_g\\ \boldsymbol{0}\end{bmatrix} \tag{75}$$

One must be careful not to ignore the cross coupling that exists between the state vector, $\boldsymbol{x}_{I,r}$ and the state vector, $\boldsymbol{x}_{I,u}$. Upon careful inspection of equation (72) one can notice that the Taylor series expansion for the relative velocity error state will have contributions from the elements of the state vector, $\boldsymbol{x}_{I,r}$. These contributions are not included in equation (75), but must be included in the implemented filtering scheme.

Combining the dynamic models for the two state vectors given in equations (44) and (75) can be written in a compact form as:

$$\delta\dot{\boldsymbol{x}}_I = \Phi_I\delta\boldsymbol{x}_I + \boldsymbol{w}_I \tag{76}$$

We must also not forget the dynamic model for the two GPS state vectors given in equations (63) and (64).

The linearized dynamic model for the GPS state vector in equation (72) can then be written in a general form as:

$$\delta\dot{\boldsymbol{x}}_G = \Phi_G\delta\boldsymbol{x}_G + \boldsymbol{w}_G \tag{77}$$

A very important difference must be pointed out between the decentralized approach shown in figure 5 and the baseline navigation algorithm shown in figure 4. The two stand-alone tightly coupled GPS/INS algorithms operating at the user and reference station provide us with a nominal state trajectory. Therefore, an extended Kalman filter does not need to be used in the decentralized algorithm. Instead, a linearized Kalman filtering scheme is used in which equations (71) and (72) serve to propagate the covariance matrix AND the state vector. That is, the states used in the integration filter are now deviation states instead of total states.

SIMULATION RESULTS

To compare the decentralized scheme to the baseline navigation algorithm, we will consider an aircraft executing a figure eight flight maneuver over a stationary reference station. The flight pattern is shown below in figure 6.

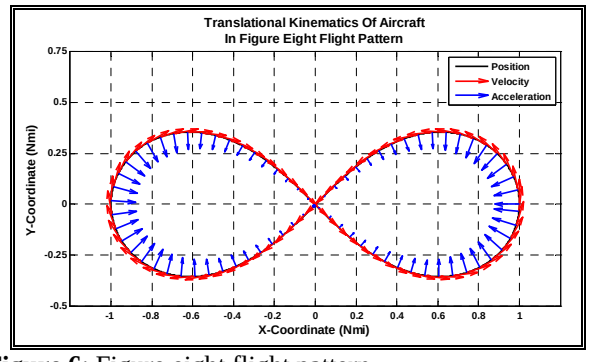

Figure 6: Figure eight flight pattern

The simulation carried out here is a Monte-Carlo simulation in which GPS ranging measurements and inertial measurements are simulated. Some pertinent parameters used in the simulation are shown in table 1 below.

Parameter	Value
Almanac	**May 2007 (30 SVs)**
Simulation location	**Chicago, Illinois**
Raw code thermal noise	**50 cm (1σ)**
Raw carrier thermal noise	**2 mm (1σ)**
Code phase multipath	**1 m (1σ)**
Carrier phase multipath	**1 cm (1σ)**
Maximum roll angle	**10 degrees**
Maximum speed	**250 knots**
Accelerometer white noise	**5 x 10^{-4} m/s^2/sqrt(Hz)**
Accelerometer bias stability	**2 x 10^{-3} m/s^2**
Gyroscope white noise	**8 x 10^{-9} rad/s/sqrt(Hz)**
Gyroscope bias stability	**2 x 10^{-6} rad/s**

Table 1: Simulation parameters

The simulation is carried out over a 1 hour period in which 8 satellites are continuously visible. Furthermore, only a floating Kalman filtering algorithm is used. No integer fixing is conducted in this paper, although this will be incorporated in ongoing research.

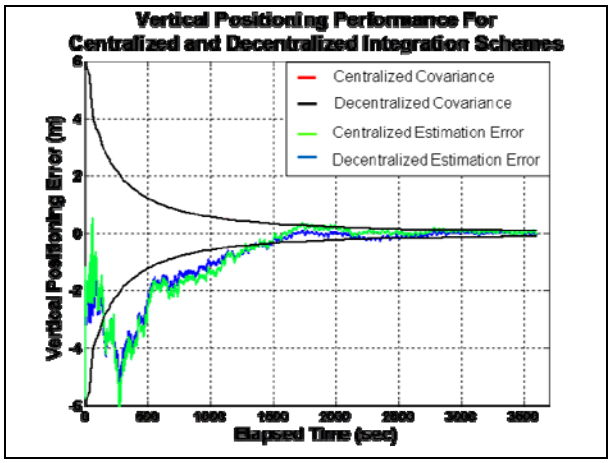

Figure 7: Simulation results

Simulation results shown in figure 7 are only for the vertical positioning error. This is done because the vertical position error is usually the worst error in relative navigation problems. We can see that for a stationary reference station, both the decentralized algorithm and the baseline navigation algorithm produce the same covariance trace. The actual estimation error is also similar for the two algorithms and converges to the correct value to within 2 centimeters. Similar results were also obtained for the north and east relative positioning solutions.

CONCLUSIONS AND FUTURE WORK

In this work a decentralized approach to tightly coupled GPS/INS integration was developed. The fundamental premise of this algorithm is that deviations of the true state from a nominal trajectory are estimated using a linearized Kalman filter. This is possible by running high rate, stand-alone tightly coupled GPS/INS algorithms separately at the reference station and user. The reference station broadcasts estimates of position and velocity to the user, who computes the nominal trajectory. The theoretical derivation of these algorithms was provided along with Monte-Carlo simulation results. Comparisons of the decentralized algorithm were made with a baseline GPS/INS algorithm where raw inertial measurements from the reference platform are theoretically available at the user platform. This simulation showed that the decentralized filtering algorithm produces a covariance envelope that closely matches the baseline algorithm for the case in which the reference station is stationary.

In future work, this algorithm will be tested using real experimental data in which satellite outages are evident. High integrity integer fixing algorithms will also be incorporated to provide real time positioning accuracy on the order of 1 cm.

ACKNOWLEDGMENTS

The authors would like to thank our sponsors at the U.S. Navy for their continued support of this research. Specifically, we would like to extend our gratitude to Marie Lage, Greg Johnson and Glen Colby for their expertise and guidance.

REFERENCES

[1] M. Heo, B. Pervan, "Carrier Phase Navigation Architecture for Shipboard Relative GPS," IEEE Trans. On Aerospace and Electronic Systems, vol. 42, no. 2, pp. 670-679, April 2006.

[2] Petovello, M.G., M.E. Cannon, G. Lachapelle, A. Huang and V. Kubacki (2004), Integration of GPS and INS Using Float Ambiguities with Application to Precise Positioning for JPALS, Proceedings of the ION NTM 2004, San Diego, CA, Jan. 2004.

[3] S. Khanafseh, B. Pervan, and G. Colby, "Carrier Phase DGPS for Autonomous Airborne Refueling," Proceedings of the Institute of Navigation 2005 National Technical Meeting, San Diego, CA, January 24-26, 2004.

[4] G. A. McGraw, T. Murphy, M. Brenner, S. Pullen, and A. J. Van Dierendonck, "Development of the LAAS Accuracy Models," Proceedings of the Institute of Navigation's ION GPS-2000, Salt Lake City, UT, September 19-22, 2000.

[5] F. C. Chan, "A State Dynamics Method for Integrated GPS/INS Navigation and It's Application To Aircraft Precision Approach," PhD Dissertation,

Illinois Institute of Technology, Chicago, IL, May, 2008.

[6] D.H Titterton, J.L. Weston, “Strapdown Inertial Navigation Technology,” The American Institute of Aeronautics and Astronautics, 2004.

[7] Jekeli, C., “Inertial Navigation Systems with Geodetic Applications”, Berlin, New York, Walter de Gruyter 2001.

[8] Farrell, Jay A, “Aided Navigation: GPS With High Rate Sensors”, New York, The McGraw-Hill Company 2008.

[9] Parkinson, Bradford W. “Global Positioning System: Theory and Applications Volume I”, Danvers Massachusetts, American Institute of Aeronautics and Astronautics, 1996.

[10] Parkinson, Bradford W. “Global Positioning System: Theory and Applications Volume II”, Danvers Massachusetts, American Institute of Aeronautics and Astronautics, 1996.

[11] Department of the Navy, “NATOPS Flight Manual Navy Model F/A – 18 E/F 165533 And Up Aircraft”, March 2001.

[12] P. Misra and P. Enge, “Global Positioning System Signals, Measurements, and Performance”. Lincoln, MA: Ganga-Jumuna Press, 2001.

[13] Wiesel, William E. “Spaceflight Dynamics”, New York, McGraw-Hill 1996.